Construction and Building Materials 166 (2018) 500–509

Contents lists available at ScienceDirect

Construction and Building Materials

journal homepage: www.elsevier.com/locate/conbuildmat

Assessment of photocatalytic, superhydrophobic and self-cleaning properties on hot mix asphalts coated with TiO_2 and/or ZnO aqueous solutions

I. Rocha Segundo [a], C. Ferreira [a], E.F. Freitas [a,*], J.O. Carneiro [b], F. Fernandes [b], S. Landi Júnior [c], M.F. Costa [d]

[a] Civil Engineering Department, University of Minho, Azurém Campus, Guimarães, Portugal
[b] Physics Department, University of Minho, Azurém Campus, Guimarães, Portugal
[c] Instituto Federal Goiano, 75901-970, Rio Verde, Goiás, Brazil
[d] Physics Department, University of Minho, Gualtar Campus, Braga, Portugal

HIGHLIGHTS

- Photocatalytic, superhydrophobic and self-cleaning capabilities were promoted on asphalt mixtures.
- AC 6 and AC 14 mixtures were coated with TiO_2 and/or ZnO aqueous solutions by spraying.
- Physicochemical and morphological properties of bitumen samples were evaluated by FTIR and AFM.
- New pavement surface capabilities assessed with Water Angle Contact and Photocatalytic Efficiency tests.
- No deterioration was guaranteed for AC 14 TiO_2, AC 14 TiO_2 ZnO, AC 6 TiO_2 and AC 6 TiO_2 ZnO solutions.

ARTICLE INFO

Article history:
Received 14 August 2017
Received in revised form 18 January 2018
Accepted 19 January 2018

Keywords:
Photocatalysis
Superhydrophobic
Self-cleaning
Asphalt mixtures
TiO_2
ZnO

ABSTRACT

Photocatalytic, superhydrophobic and self-cleaning capabilities were promoted on AC 6 and AC 14 asphalt mixtures by spraying of TiO_2 and/or ZnO. Initially, physicochemical and morphological properties of bitumen samples were evaluated by Fourier Transform Infrared Spectroscopy and Atomic Force Microscopy after the solution spraying of TiO_2, ZnO and TiO_2 ZnO. Then, to assure those capacities, Water Angle Contact and Photocatalytic Efficiency tests were carried out on both mixtures. Finally, mixtures were assessed mechanically through Indirect Tensile Strength. Photocatalytic, superhydrophobic and self-cleaning properties were guaranteed for AC 14 with TiO_2 and TiO_2 ZnO and AC 6 with TiO_2 ZnO without deteriorations.

1. Introduction

Nowadays air pollution is one of the biggest problems in the world in developing and developed countries, mainly in urban and industrial areas. Some consequences in different scales can be related with the air pollution: intensification of greenhouse effect, acid rain and public health problems. In general, the road transportation is the most important responsible of the environmental pollution in urban areas. This pollution causes a lot of human health problems to the society [1,2]. Photocatalytic materials applied in civil construction market can mitigate this problem, photodegrading pollutants, manly NO_x and SO_2 [3–5].

Road pavements must have essentially the capacity to resist to traffic and climate efforts and to guarantee rolling conditions: safety, comfort and economic issues. The functionalization of materials is the act of modifying materials in order to provide new capabilities, usually to their surface. In asphalt mixtures, these new multifunctional capabilities will be promoted by the photocatalytic oxidation of pollutant agents and self-cleaning property, contributing to the purification of the air and degrading of organic pollutants. The need of large areas to catch pollutants is a good reason to provide roads with the photocatalytic capacity.

Related to safety, one of the most important superficial characteristics of pavements is friction. Friction drops significantly when

* Corresponding author.
E-mail addresses: iran_gomes@hotmail.com (I. Rocha Segundo), eng.cristiano.ferreira@gmail.com (C. Ferreira), efreitas@civil.uminho.pt (E.F. Freitas), carneiro@fisica.uminho.pt (J.O. Carneiro), f_daniela_06@hotmail.com (F. Fernandes), salmon.landi@ifgoiano.edu.br (S.L. Júnior), mfcosta@fisica.uminho.pt (M.F. Costa).

https://doi.org/10.1016/j.conbuildmat.2018.01.106
0950-0618/

there is water or ice on the pavement surface. Thus, it is important to drain or repel the surface water quickly. Superhydrophobic materials can repel the water very quickly and the self-cleaning property provides the superficial cleaning [6–9]. According to Wenzel (1936), the wettability of a surface can be explained by a thermodynamic process, so two cases are considered: (i) hydrophilic surface: spontaneous process that the free energy of the wet interface is smaller than the free energy of dry interface; (ii) hydrophobic surface: non-spontaneous process that the free energy of dry interface is lower than the free energy of wet interface. There are two models for measuring the surface wettability: (i) Wenzel's model (1936): water droplets penetrates the microgeometry features of surface roughness; (ii) Cassie-Baxter's Model (1945): water droplets are suspended on the surface roughness by the air between them [8]. The superhydrophobic functionalization was already developed in asphalt mixtures with polytetrafluoroethylene (PTFE) with water contact angle up to 166° [9] and with copolymer fluoroacrylate modified with CaO nanoparticles with water contact angle 163° [8].

The presence of oil, grease and dirty particles on the pavement also reduces significantly friction [10,11]. The self-cleaning property can reduce accidents in oil spilled areas and also in dusty areas. It is possible due to major capabilities: water droplets roll and carry the dirt previously deposited cleaning the superhydrophobic surfaces [7]; and, photocatalytic materials can degrade organic pollutants like oil and greases [12].

The semiconductor TiO_2 is the most used material to provide the photocatalytic capacity in asphalt mixtures' researches [1,12–15]. It is important to improve and evaluate this new capacity by testing other semiconductors, like ZnO and the combination of these two semiconductors in order to improve the photocatalytic and self-cleaning capacities of the asphalt mixtures, mitigating air pollution and reducing accidents. TiO_2 and ZnO have low toxicity and cost and high stability and availability providing a powerful oxidation [16,17].

The photocatalytic process is described by six reactions [15,18–20]. The process begins with irradiating the semiconductors with UV light. When the semiconductor absorbs an energy equal to or superior than the band gap, an electron is transferred from valence band to the conduction band (Eq. (1)).

$$TiO_2 \xrightarrow{hv} h^+ + e^- \quad (1)$$

In this reaction, h^+, which has great reducing power, reacts with water (moisture) to generate hydroxyl (OH^*), which also presents high oxidizing power. On the other hand, e^- accomplishes the reduction of oxygen molecule to produce superoxide anion (O_2^-), which is very effective on pollutant' degradation (Eqs. (1) and (2)).

$$h^+ + OH^- \rightarrow OH^* \quad (2)$$

$$e^- + O_2 \rightarrow O_2^- \quad (3)$$

The O_2^- reacts with H^+, dissociation from water, and forms HO_2 (Eq. (3)). From these radicals, pollutants gases, mainly NOx, are degraded. The final product, HNO_3, can be washed by rainwater (Eqs. (5) and (6)).

$$H^+ + O_2^- \rightarrow HO_2^* \quad (4)$$

$$NO + HO_2^* \rightarrow NO_2 + OH^* \quad (5)$$

$$NO_2 + OH^* \rightarrow HNO_3 \quad (6)$$

It is relevant to study the effect of the asphalt substrates (different asphalt mixtures) on the photocatalytic process. Therefore, in this research the morphologic and chemical properties of asphalt bitumens were analyzed after spraying of different semiconductors on samples to verify if the use of this technique did not damage the bitumen, in a first stage. In a second stage, the photocatalytic efficiency and the wettability of asphalt mixtures were evaluated after spraying with aqueous solutions of: TiO_2; ZnO; and, a combination of TiO_2 and ZnO. To guarantee that the effect still occurs after traffic, the asphalt mixture samples were submitted to an abrasion process explained in Chapter 2.2. Finally, the effect of the best aqueous solution on mechanical properties of asphalt mixture samples was assessed.

2. Materials and methods

2.1. Materials

In order to develop the research two bitumens were used: Cepsa® 35/50 and Elaster® 13/60, from Cepsa company, to compose two asphalt mixtures: AC 14 surf 35/50 and AC 6 surf Elaster 13/60 respectively. In order to functionalize these materials two semiconductors were used: nano-TiO_2 by Quimidroga (Aeroxide TiO_2 P25: 80% and 20% rutile); and, micro-ZnO by Sigma Aldrich.

The results of the bitumen characterization are presented in Table 1.

The band gap of the semiconductors was measured by diffuse reflectance and calculated using the Kubelka-Munk equation [21,22]. This energy necessary to start the reaction is 3,20 eV for TiO_2 and 3,25 eV for ZnO, corresponding to UV-A light.

Three aqueous solutions were prepared with: TiO_2 nanoparticles (4 g/L); ZnO microparticles (1 g/L); and TiO_2 nanoparticles (4 g/L) + ZnO microparticles (1 g/L). The aim was to improve the photocatalytic efficiency by combining semiconductors to decrease the band gap (by doping) to trigger the photocatalytic property. All the solutions had pH 8 in order to prevent any negative impact into the bitumen and guarantee less aggregate agglomeration of the semiconductors [12].

The asphalt mixes were prepared following the standard EN 13108-1 and their temperatures of production and compaction following the bitumen curve viscosity *versus* temperature. The AC 6 mixture is characterized by an uniform granulometry, it is composed mostly by intermediate aggregates (4/6) and commercial asphalt bitumen which is modified by SBS. It also has a high volume of voids (10.9%). The AC 14 mixture is a conventional asphalt mixture that shows a dense granulometry, is composed by conventional asphalt bitumen 35/50 and has low volume of voids (4.7%). Both mixtures are used as structural and functional pavement layers but AC 6 has a very limited structural impact. Often it is used when improved superficial characteristics are required. The samples were compacted in two geometries: cylindrical following Marshall Design that is used to analyze the mechanical impact of the semiconductors; and, prismatic slabs by rolling compaction used to be cut and then to analyze the wettability and photocatalytic efficiency. The main characteristic of the AC 6 and AC 14 asphalt mixes of the slabs are given in the Table 2.

For Marshall samples, used to analyze the mechanical impact of semiconductors, AC 6, compacted with 50 blows in each surface, presented a VC of 9.2%, and the AC 14, compacted with 75 blows in each surface, had a VC of 4.8%. The volume of voids of the mixtures was similar and independent of the geometry.

Table 1
Properties of the Bitumens.

Properties	35/50	Elaster	Test specification
Softening point/°C	56	63	ASTM D 36
Penetration at 25 °C/0.1 mm	30	46	ASTM D 5
Brookfield viscosity at 145 °C/Pa s	0.5607	1.2109	ASTM D 4402

Table 2
Properties of Asphalt Mix Slabs.

Asphalt Mix	Filler (%)	Fine Aggregates 0/4 (%)	Intermediate Aggregates 4/6 (%)	Intermediate Aggregates 4/8 (%)	Coarse Aggregates 6/14 (%)	Bitumen (%)	Maximum Bulk Density (g/cm^3)	Voids content (VC) (%)
AC 6	3	25	72	–	–	6	2.423	10.9
AC 14	3	41	–	12	44	5	2.474	4.7

2.2. Sample preparation

The method of application of the semiconductors was by spraying an aqueous solution onto the surface of the asphalt mixtures. This is the most efficient method when compared with others methods such as volume incorporation or bitumen modification [1,12,23]. This method consists of spraying the aqueous solution with an atmospheric air compressor at a distance of about 20 cm during 30 s, being the speed of the aqueous solution jet set at 100 mL/min, thus leading to coverage rates of around 5 mg/cm^2 to 12.5 mg/cm^2. The temperature of the asphalt mixes at spraying was 60 °C, which is similar to the softening point temperature of both bitumens.

In this research 2 approaches were carried out: analysis of the bitumens sprayed directly with the semiconductors; and, analysis of the asphalt mixtures sprayed with the semiconductors.

The bitumen damage/deterioration caused by the semiconductors was evaluated when applied directly onto bitumen samples. A hot drop of bitumen was carefully deposited on a glass microscope slide substrate, and spread out with a blade to form a film that covered the glass surface. Then the aqueous solutions were applied by spraying. Fourier Transform Infrared Spectroscopy (FTIR) and Atomic Force Microscope (AFM) results were compared including samples without treatment for control. The samples that were analyzed by FTIR were covered by a plastic film to protect the equipment.

In order to evaluate the photocatalytic property and efficiency, the solutions were applied in prismatic samples ($25 \times 25 \times 15$ mm^3) cut from slabs. These samples were used to evaluate the water contact angle and the photocatalytic efficiency. To evaluate the semiconductors' fixation, the tests were carried out before and after abrasion using a metallic wire brush disc (at 200 RPM) conducting in 3 mass loss levels of the samples: 0,25%, 0,50% and 1%. The abrasion was carried out homogeneously over the asphalt mixtures' surface.

Finally, the best aqueous solution was applied to the asphalt mixes AC 6 surf Elaster 13/60 and AC 14 surf 35/50 Marshall samples to evaluate if there is a moisture impact into their mechanical properties. The Fig. 1 shows the procedure used to prepare the samples for testing.

2.3. Methods

2.3.1. Atomic Force Microscopy (AFM)

To study the bitumen surface morphology sprayed with semiconductors, the samples were evaluated by AFM. The structures of bitumen observed in this evaluation are: (i) *catana phase* or bee structures (pale lines as peaks and back lines as valleys). This phase could be related with the asphaltenes [24–26]; (ii) *periphase* pale region around the *catana* phase; (iii) *perpetual* phase: structural matrix. The samples were scanned over lengths of 5 μm to give a surface area of 25 μm^2 using the equipment Digital Instruments NanoScope III Atomic Force Microscope. The absence of the catana phase could indicate a superficial change in the bitumen, due to the degradation of the asphaltenes [12].

2.3.2. FTIR

Fourier Transform Infrared Spectroscopy (FTIR) was performed to analyze the bitumens sprayed with semiconductors and the control sample. The FTIR spectrum was recorded on an Avatar 360 FTIR system, Nicolet, 4000–400 cm^{-1} spectral range, equipped with multi-bounce HATR and diffusion reflectance accessories. The semiconductors and bitumens' spectrums will be presented in Chapter 3.2.

2.3.3. Water contact angle (WCA)

The Water Contact Angle (WCA) test was carried out to evaluate the wettability of asphalt pavement and characterize its hidro phylicity/hydrophobicity. To measure this property Cassie-Baxter's model was considered because the water drop would be probably suspended on surface roughness, justified by the rough and hydrophobic surface [8]. Using the equipment OCA 15 plus Dataphysics, 3 readings of 5 μL water drops were carried out at 3 samples during 30 min, at room temperature and relative humidity, and the arithmetic mean was calculated. The analysis of variance (ANOVA) and PostHoc statistical test were done to evaluate the different parameters and their influence in the Water Contact Angle.

2.3.4. Photocalytic efficiency evaluation

The new capabilities of materials on test, photocatalytic and self-cleaning, can be evaluated by the degradation of a dye [27,28]. It was carried out with the functional asphalt mixes by measuring the maximum absorption of Rhodamine B (RhB) (554 nm^{-1}) (using a Shimadzu 3101 PC spectrophotometer) with concentration of 5 ppm (pH 5) as a function of a light that simulates the sun irradiation (with a power intensity of 11 W/m^2, measured with a Quantum Photo Radiometer HD9021 Delta Padova) in different times. Each sample was immersed in 30 mL of RhB aqueous solution distant 25 cm from the light. After 6 h in dark condition (adsorption), the samples were irradiated with a 300 W - OSRAM UltraVitalux lamp. In order to avoid the evaporation of RhB solution that can increase the concentration, all the systems were closed with a transparent plastic film with at least 90% of transmittance in the wavelength range between 292 and 900 nm. The photocatalytic efficiency (Eq. (7)) was calculated using the Beer–Lambert law [12]. Also ANOVA and Post Hoc test were done to evaluate better the photocatalysis results.

$$\Phi(\%) = \left(\frac{A_o - A}{A_o}\right) \times 100 \tag{7}$$

where Φ is the photocatalytic efficiency; A and A_0 represent the maximum absorbance of RhB solution for time t and 0 h, respectively.

2.3.5. Mechanic impact of semiconductors

To analyze the mechanical impact of the functionalized asphalt mixtures, tests of Indirect Tensile Strength (ITS) were carried out according to the standard EN 12697-23. Two groups of three samples were evaluated with and without TiO_2 + ZnO semiconductors after water immersion process. This water process was carried out

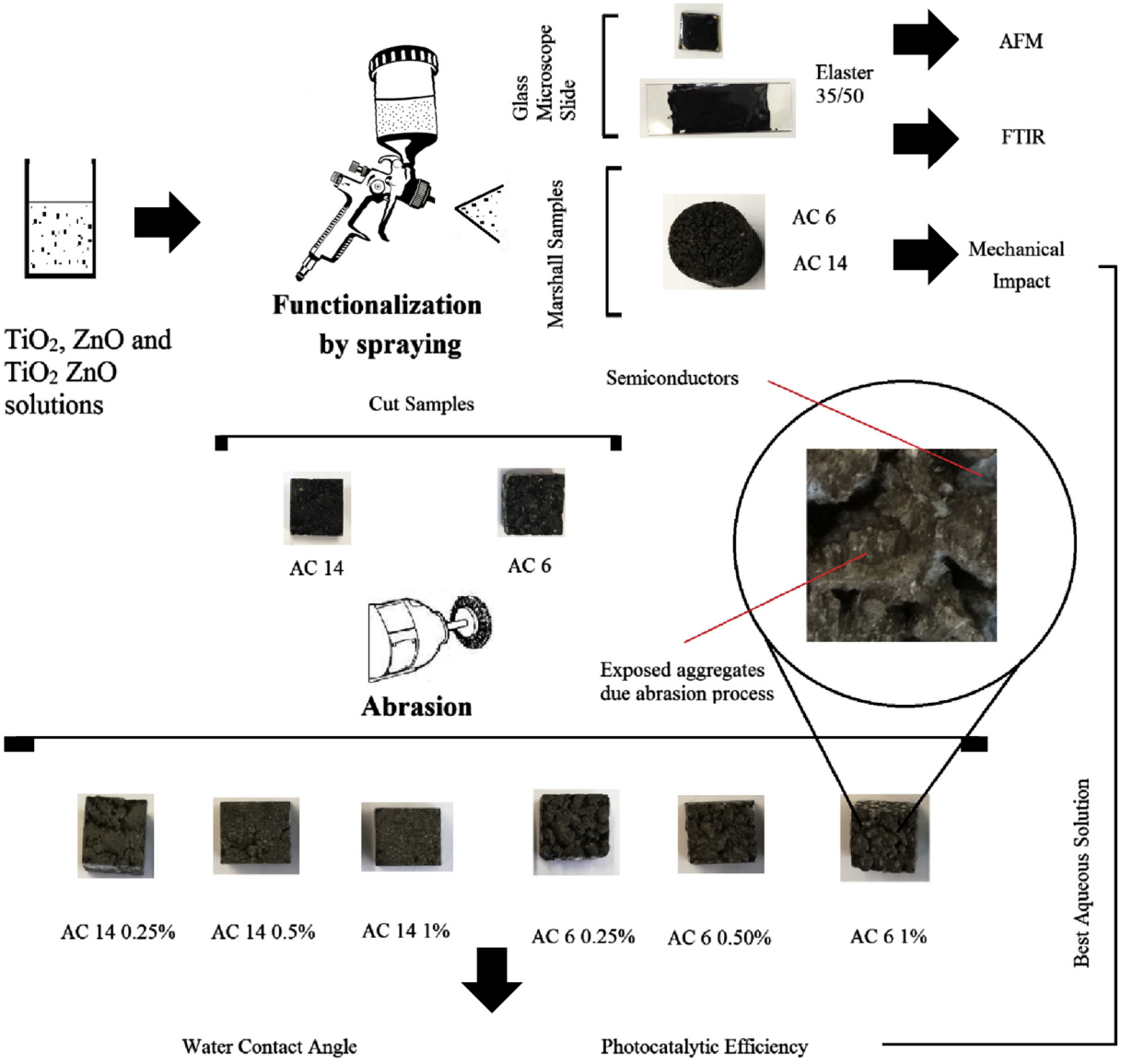

Fig. 1. Sample preparation for AFM, FTIR, mechanical impact, water contact angle and photocatalytic efficiency measurements.

due to different wettability of the materials which could cause different mechanical impacts. The parameter Resistance Index (*RI*), which is the ratio of the difference of the resistances of functionalized samples (ITS_f) and the not functionalized samples (*ITS*) to *ITS* (Eq. (8)), was calculated.

$$RI = \frac{ITS_f - ITS}{ITS} \tag{8}$$

3. Results

3.1. Atomic Force Microscopy (AFM)

Fig. 2 shows the AFM results. The absence of the catana phase could indicate a superficial alteration in the bitumen, that is, the degradation of the asphaltenes [12]. The bee structures were identified in the bitumen without the presence of semiconductors and after TiO_2 and TiO_2 + ZnO application. The ZnO solution presents an impact on the bitumen surface explained by the absence of the structure, indicating a superficial degradation of the bitumens.

3.2. Fourier Transform Infrared Spectroscopy (FTIR)

Fig. 3 shows the FTIR of bitumens with and without semiconductors. In the commercial Elaster bitumen when comparing with the bitumen 35/50 an accentuation is noticed in the peaks referring to the butadiene: 959.55 cm^{-1}, to the styrene: 684.76 cm^{-1}, both referring to SBS, and the aromatic C—H vibration [29]. For both bitumen, peaks 2923.11 and 2860.79 cm^{-1} are respectively related to the vibration of the asymmetric C—H (CH_3 and CH_2) shift and the symmetrical C—H (CH_3 and CH_2) stretching. Peak 1596.46 cm^{-1} is related to vibrations of aromatic C=C and C—H elongation and peak 1431.68 cm^{-1}, with C—H flexion.

It is possible to note that the ZnO solution sprayed onto the Elaster bitumen showed higher impact on this bitumen, having an impact on the transmittance of the functional groups. Differently

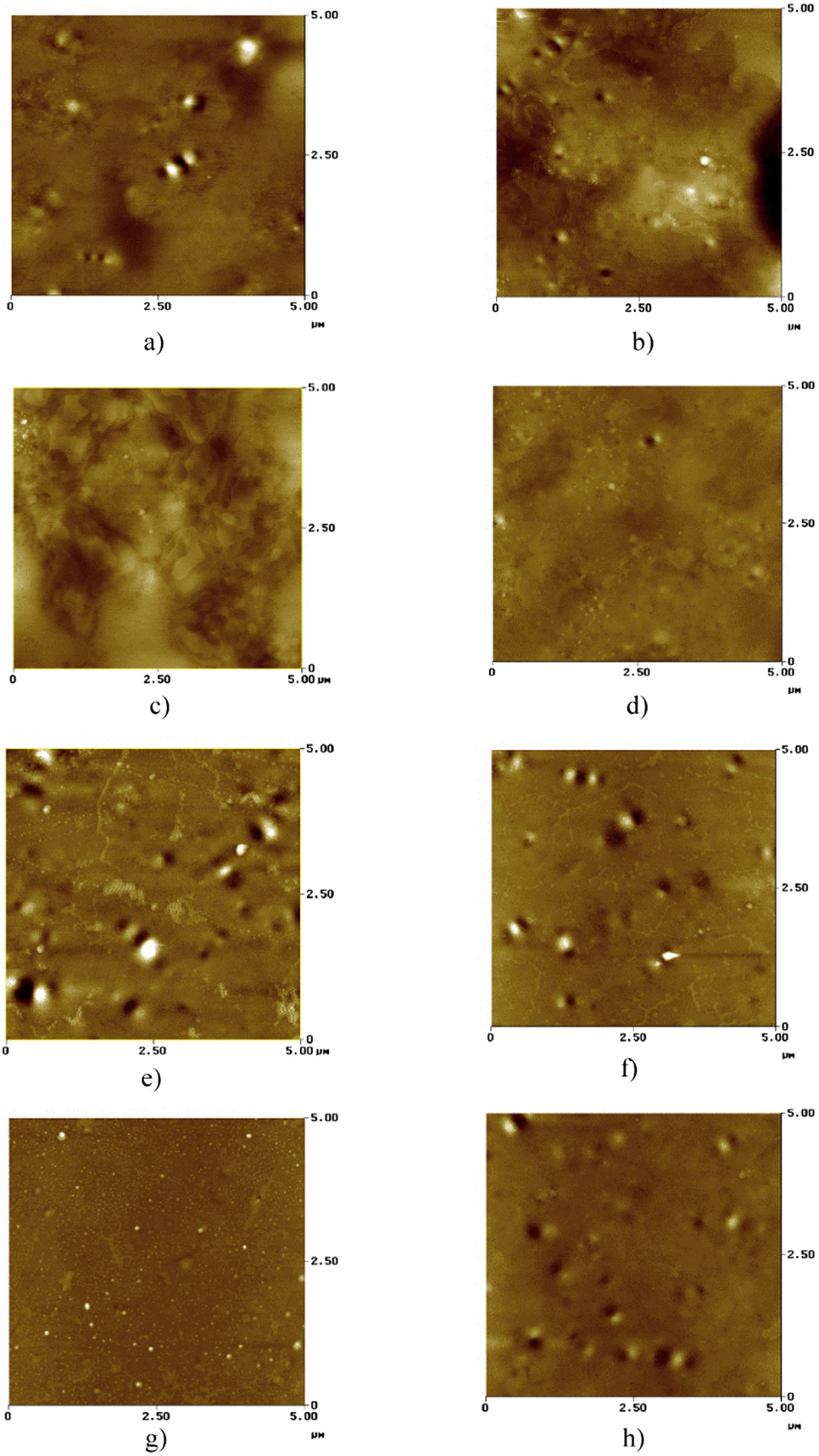

Fig. 2. AFM Results: (a) Cepsa 35/50; (b) Cepsa 35/50 + TiO_2; (c) Cepsa 35/50 + ZnO; (d) Cepsa 35/50 + TiO_2 + ZnO; (e) Elaster 13/60; (f) Elaster 13/60 + TiO_2; (g) Elaster 13/60 + ZnO; (h) Elaster 13/60 + TiO_2 + ZnO.

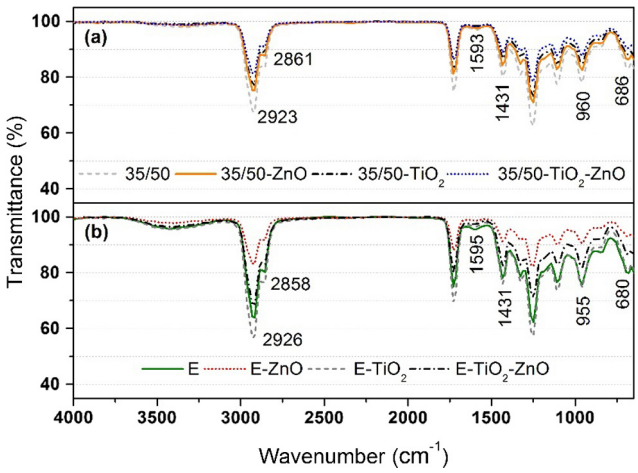

Fig. 3. FTIR of 35/50 and Elaster (E) before and after the application of semiconductors.

from the Elaster, the bitumen 35/50 showed little change in its spectrum.

3.3. Water contact angle analysis

Fig. 4 shows the results of water contact angle (wettability) of the asphalt mixtures with the different treatments and wear levels. The initial contact angle for the mixtures before abrasion was higher than after abrasion. In general, after this first moment the result was the opposite. Initially, the aggregates at the surface of the mixtures were covered with bitumen, resulting in a smooth surface, therefore contributing to the lower contact angle. With abrasion, the microtexture of the aggregates was exposed, increasing the roughness of the surface and consequently the water contact angle. Taking this into account, in the beginning of the life time of the pavements, the natural removal of the bitumen film due to tyre wear is important to increase not only friction but also hydrophobicity.

For both mixtures, the higher initial contact angle was found for the samples treated with TiO_2 and ZnO. The superhydrophobicity, WCA higher or equal to 150° was guaranteed for the mixtures AC 14 TiO_2, AC 14 TiO_2 ZnO and AC 6 TiO_2 ZnO. The initial WCA is the most important angle because the water drains in a very short time to the roadside. The lower WCA was obtained for AC 14 without treatment after 1% of abrasion (108°) and AC 6 without neither treatment nor abrasion (102°).

After 30 min, it was possible to have WCA equal or higher than 40° for AC 14 ZnO 0.25% (63°), AC 14 TiO_2 ZnO (51°), AC 6 TiO_2 0.25% (40°), AC 6 ZnO 0.25% (40°) and AC 6 TiO_2 ZnO 0.25% (40°). On the other hand, the sample AC 14 without treatment and abrasion had the lowest WCA, below 10°. Table 3 summarizes the maximum and minimum results for Water Contact Angle.

An analysis of variance, ANOVA (factors: abrasion, treatment, time, mixture), was carried out to determine if there is an interaction effect between the independent variables over the water contact angle for a significance level of ($1 - \alpha = 0.1$). This parameter indicates the risk (%) of concluding that an effect exists when there is no actual effect. Table 4 shows the ANOVA results: Fisher (F value) and p-value. Mixture ($p < 0.001$), Time ($p < 0.001$), Treatment ($p < 0.001$) and Abrasion ($p < 0.1$) had a significant influence on contact angle measurements. Only the interactions of the following variables had a significant effect on the dependent variable results: i) Mixture and Treatment ($p < 0.001$); ii) Mixture and abrasion ($p < 0.01$); iii) Treatment and Abrasion ($p < 0.001$); iv) Mixture, Time and Treatment ($p < 0.01$).

The Bonferroni Post-Hoc test for a level of significance ($1 - \alpha = 0.1$) has the following factors:

3.3.1. Factor 1 - Time

The average of the contact angle for time equal to zero were higher when compared to that of times equal to 0.3333 s ($p < 0.001$). The averages of the contact angle of the times 0.6666 and 0.3333, 1 and 0.3333, 1 and 0.6666, 2 and 0.6666, 2 and 1, 3 and 1, 3 and 2, 4 and 2, 4 and 3, 5 and 2,5 and 3, 5 and 4 did not present significant differences in average of contact angle ($p > 0.1$). For all other times, the difference of the averages of the contact angle were significant ($p < 0.1$). It can be concluded that the initial WCA is the most important.

3.3.2. Factor 2 - Treatment

The average of the WCA measurements of the treated samples were significantly higher when compared to the untreated samples ($p < 0.001$), but the averages of the WCA of the treated samples did not differ significantly. Therefore, the hydrophobicity was higher for the treated samples compared to the non-treated ones.

3.3.3. Factor 3 - Abrasion

The averages of the WCA measurements of the worn samples were significantly different from the average of the samples without abrasion: 0.25% ($p < 0.001$); 0.5% ($p < 0.001$) and 1% ($p < 0.05$). Only the WCA averages for the samples with 0.25% and 1% wear level differ significantly ($p < 0.05$). It can be concluded that WCA for consecutive wear levels were similar.

3.3.4. Factor 4 – Asphalt Mixture

The average of WCA measurements of the AC 14 samples was significantly lower than the AC 6 samples ($p < 0.001$).

3.4. Photocatalytic efficiency

Fig. 5 shows the results of photocatalysis for the asphalt mixtures. During 6 h, the samples were submerged inside the dye solution in dark condition in order to analyze the adsorption without photodegradation reactions. When the adsorption was constant, the light was turned on.

After 8 h of irradiation, the best results for photocatalytic efficiency were achieved for the samples treated with TiO_2 (57%) and TiO_2 ZnO (56%) for AC 14 and TiO_2 ZnO for AC 6 (49%). The results show that the combination of these materials was more efficient for AC 6 due to the increase of 18% on the photocatalytic efficiency comparing with the results only with TiO_2. AC 14 did not have any impact when combining the semiconductors. After abrasion, the worst situation was found for AC 14 treated with ZnO, which show a decrease, on average, of 59%. For AC 6, it was a decrease of 48%. The best fixation of semiconductors was for AC 6 TiO_2, with a decrease of 8% in photocatalytic efficiency comparing with the average of the worn samples.

The results after 24 h of irradiation, done only for the samples before abrasion, show that the mixture before treatment has 29% and 36% of photocatalytic efficiency for, respectively, AC 14 and AC 6 samples. Probably this was caused by a presence of semiconductors in the aggregates exposed due to sample cutting.

It was possible to achieve photocatalytic efficiencies of 79% for AC 14 ZnO, up to 92% for AC 14 TiO_2 ZnO and 57% for AC 6 ZnO, and up to 81% for AC 6 TiO_2 ZnO samples. After doping, when the semiconductors were combined, the results showed an increase of 8% for AC 14 and 13% for AC 6 comparing with the samples treated only with TiO_2.

Analyzed by a variance analysis (ANOVA) for a confidence level of ($1 - \alpha = 0.1$), the results of the independent variables Mixture ($p < 0.01$), Time ($p < 0.001$), Treatment ($p < 0.001$) and Abrasion ($p <$

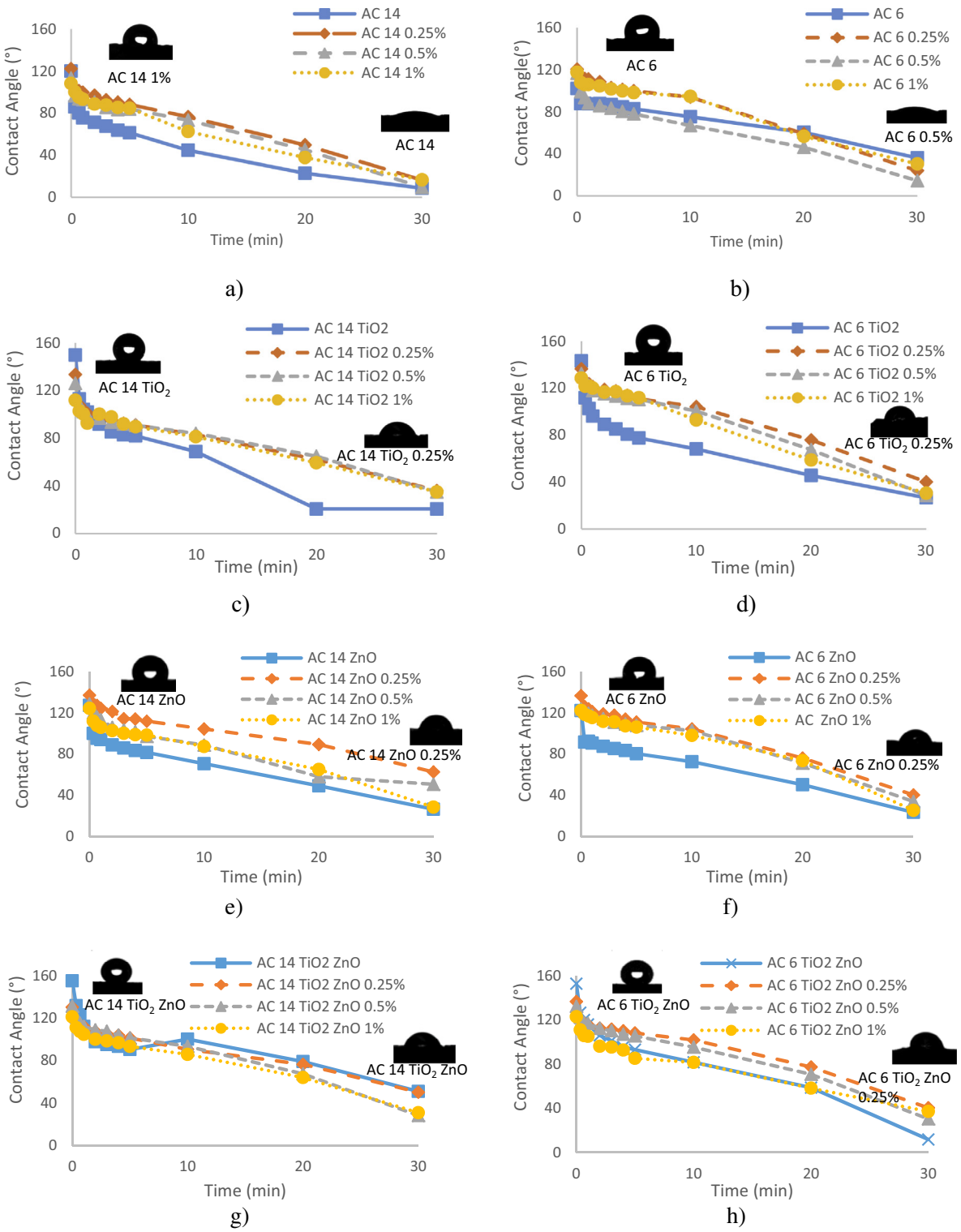

Fig. 4. Water Contact Angle: (a) AC 14; (b) AC 6; (c) AC 14 TiO_2; (d) AC 6 TiO_2; (e) AC 14 ZnO; (f) AC 6 ZnO; (g) AC 14 TiO_2 ZnO; (h) AC 6 TiO_2 ZnO.

0.001) have a significant influence on the measurements of the photocatalytic efficiency (Table 5). The interactions of the following variables had a significant impact on the results of the photocatalysis: i) Mixture and Treatment ($p < 0.01$); ii) Mixture and Abrasion ($p < 0.05$); iii) Treatment and Abrasion ($p < 0.1$); iv) Time and Abrasion ($p < 0.001$); v) Mixture and Time ($p < 0.1$) and vi) Time and Treatment ($p < 0.001$). The interaction between the combinations of three independent variables has a significant influence on the measurements of the photocatalytic efficiency ($p < 0.1$).

The Bonferroni Post-Hoc test for a level of significance ($1 - \alpha = 0.1$) has the following factors:

3.4.1. Factor 1 - Time

The average of the photocatalytic efficiency at 0.5 h and 1 h did not differ significantly. The average of the photocatalytic efficiency at 1 h and 2 h presented significant differences ($p < 0.05$). For all the other times, the average of photocatalytic efficiency differed

Table 3
Maximum and Minimum Results for Water Contact Angle.

Mixture	Treatment	Maximum WCA				Minimum WCA			
		Initial		Final		Initial		Final	
		Abrasion (%)	WCA (°)	Abrasion (%)	WCA (°)	Abrasion (%)	WCA (°)	Abrasion (%)	WCA (°)
AC 14	–	0.25	122	1.00	17	1.00	108	–	9
	TiO_2	–	**150**	0.25	36	1.00	112	–	21
	ZnO	0.25	137	0.25	63	1.00	124	–	26
	TiO_2 ZnO	–	**155**	–	51	1.00	121	0.50	28
AC 6	–	0.25	120	–	36	–	102	0.50	14
	TiO_2	–	143	0.25	40	1.00	129	–	27
	ZnO	0.25	136	0.25	40	–	122	–	23
	TiO_2 ZnO	–	**153**	0.25	40	1.00	123	–	12

Bold values indicate Water Contact Angles above 150º.

Table 4
Results of ANOVA for Contact Angle.

Variables	F value	p-value	
Mixture	107.800	<0.001	***
Time	2248.411	<0.001	***
Treatment	90.119	<0.001	***
Abrasion	3.245	0.072	.
Mixture and Time	0.048	0.826	
Mixture and Treatment	12.822	<0.001	***
Time and Treatment	0.726	0.536	
Mixture and Abrasion	10.022	0.002	**
Time and Abrasion	0.978	0.323	
Treatment and Abrasion	10.003	<0.001	***
Mixture, Time and Treatment	4.821	0.002	**
Mixture, Time and Abrasion	1.546	0.214	
Mixture, Treatment and Abrasion	0.341	0.711	
Time, Treatment and Abrasion	1.126	0.337	
Mixture, Time, Treatment and Abrasion	1.907	0.149	

. $p < 0.1$, * $p < 0.05$, ** $p < 0.01$, *** $p < 0.001$

significantly with $p < 0.01$. This means, as expected, that the photocatalytic efficiency increases during the time irradiation.

3.4.2. Factor 2 - Treatment

The average of the photocatalytic efficiency between treated samples and non-treated samples presented significant differences ($p < 0.01$), except for the samples treated with ZnO. In addition, the average photocatalytic efficiency of samples treated with TiO_2 ($p < 0.01$) and TiO_2 ZnO ($p < 0.01$) differs significantly from samples treated with ZnO. It is important to emphasize that the average of the photocatalysis results of the samples treated with TiO_2 did not differ significantly from the samples treated with TiO_2 ZnO. The average of the samples treated with ZnO did not differ significantly from the samples without treatment. Therefore, it can be concluded that the use of ZnO did not have any improvement separated or combined with TiO_2 regarding only the photocatalytic properties.

3.4.3. Factor 3 - Abrasion

The average of the photocatalytic efficiency of the samples before abrasion were significantly higher than the one of the samples at 0.5% ($p < 0.05$) and at 1% ($p < 0.001$), but not at 0.25%. However, the average of photocatalytic efficiency between the worn samples does not differ significantly between them. Low levels of abrasion do not effect photocatalytic efficiency.

3.4.4. Factor 4 – Asphalt Mixture

The average of the photocatalytic efficiency of the different bituminous mixtures samples does not differ significantly. Therefore, the functionalization, taking into account the photocatalytic property, does not have influence on the substrate of different asphalt mixtures.

3.5. Mechanic impact of semiconductors

The mechanical impact of the semiconductors on the mixture was assessed trough Indirect Tensile Strength after immersing the samples in water. The Resistance Index (*RI*) was for AC 6, −2.9% and, for AC 14, 0.1%. After the semiconductors application, the asphalt mixtures had almost the same performance. Therefore, it can be concluded that the best aqueous solution of semiconductors, TiO_2 ZnO, applied by spraying had no mechanical impact.

4. Conclusions

This study aimed at developing and accessing photocatalytic, superhydrophobic and self-cleaning asphalt mixtures sprayed with TiO_2 or/and ZnO aqueous solutions. In the first stage bitumen samples were chemically and morphologically assessed in order to analyze if there was any bitumen deterioration after the solution spraying. Next, two types of asphalt mixtures functionalized with TiO_2 ZnO were assessed mechanically through indirect tensile strength after water immersion in order to find out if there were mechanical impacts caused by the semiconductors. Finally, the samples were evaluated by Water Angle Contact and by photocatalytic efficiency to analyze these new capabilities. Eight conditions of mixtures and semiconductors were evaluated: a) AC 14; b) AC 6; c) AC 14 TiO_2; d) AC 6 TiO_2; e) AC 14 ZnO; f) AC 6 ZnO; g) AC 14 TiO_2 ZnO; h) AC 6 TiO_2 ZnO. The results of the experimental activity leaded the following conclusions:

- Based on AFM, ZnO affects the bitumen physical integrity. The bee structure, or catana phase, disappeared. This is indicative of bitumen deterioration. The other solutions, with TiO_2 and TiO_2 ZnO, maintained the integrity of the bitumen.
- The FTIR showed on the one hand a high impact of the ZnO solution sprayed on the Elaster bitumen, and, on the other hand, little impact on the conventional 35/50 bitumen.
- The wettability of asphalt pavement and its hidrophylicity/hydrophobicity were evaluated by Water Contact Angle (WCA). The initial WCA before abrasion was higher than after. In general, for later times the relation was the opposite. The superhydrophobic property was developed for these samples: AC 14 TiO_2, AC 14 TiO_2 ZnO and AC 6 TiO_2 ZnO (WCA higher or equal to 150°). Therefore, the combination of TiO_2 and ZnO was important to achieve the superhydrophobic property.
- The use of TiO_2 aqueous solution sprayed onto the surface of the asphalt mixtures was able to promote the photodegradation of an organic pollutant (Rhodamine B dye – RhB). After 24 h of light irradiation, the maximum photocatalytic efficiency (92%) was obtained for samples functionalized with TiO_2 and doped with ZnO. After 8 h of irradiation, the worst situation was for

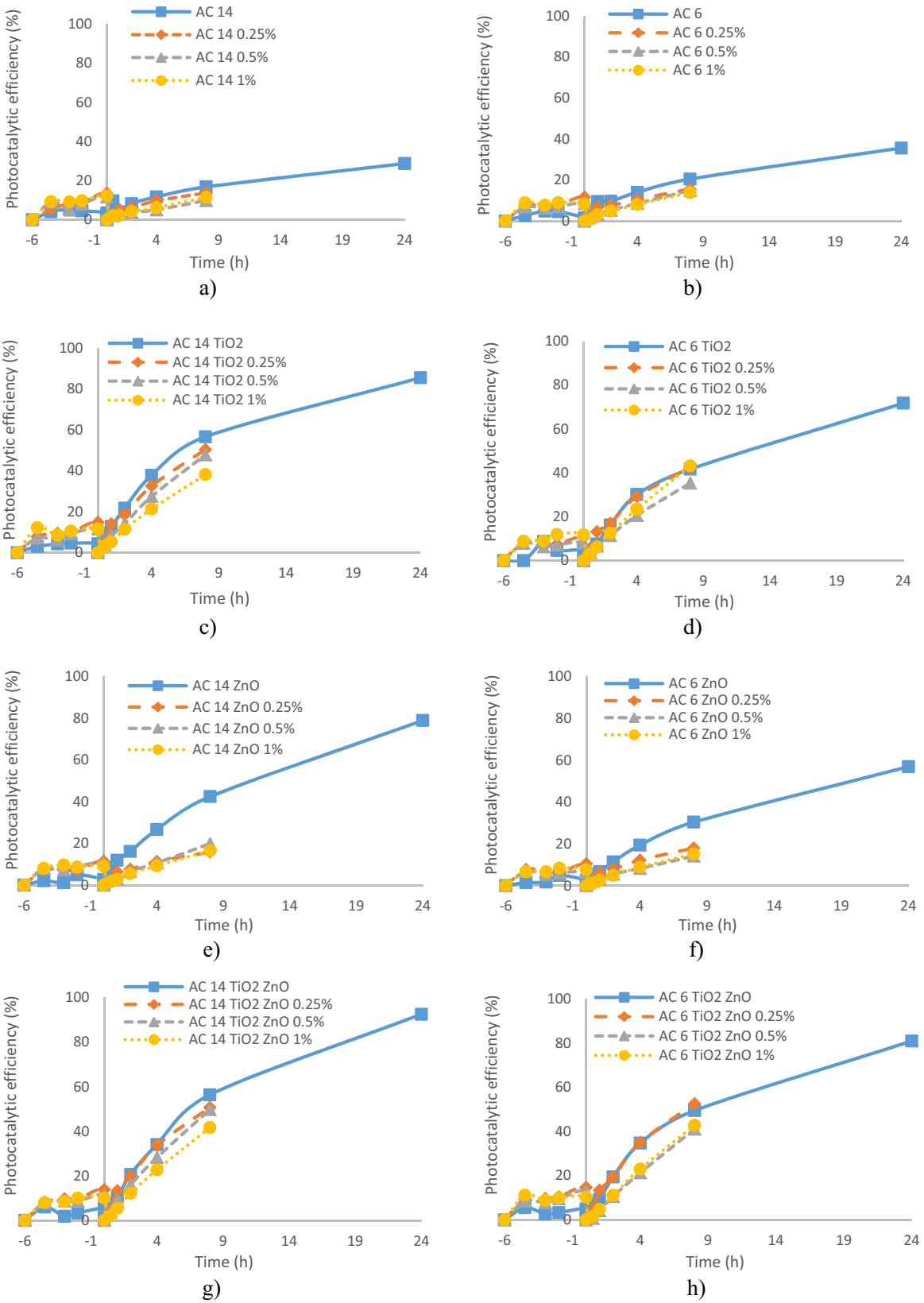

Fig. 5. Photocatalytic Efficiency: (a) AC 14; (b) AC 6; (c) AC 14 TiO_2; (d) AC 6 TiO_2; (e) AC 14 ZnO; (f) AC 6 ZnO; (g) AC 14 TiO_2 ZnO; (h) AC 6 TiO_2 ZnO.

AC 14 ZnO, which had after abrasion a decrease in average of 59% of the photocatalytic efficiency, and the best situation, AC 6 TiO_2, which has a decrease in average of 8%. After analysis of Bonferroni Post-Hoc test, the use of ZnO is not recommended to promote the photodegradation neither separated nor in combination with TiO_2.

Table 5
Results of ANOVA for Photocatalytic Efficiency.

Variables	F value	p-value	
Mixture	10.708	0.001	**
Time	1519.445	<0.001	***
Treatment	166.017	<0.001	***
Abrasion	133.830	<0.001	***
Mixture and Time	3.302	0.070	.
Mixture and Treatment	4.899	0.002	**
Time and Treatment	114.958	<0.001	***
Mixture and Abrasion	5.813	0.016	*
Time and Abrasion	11.384	<0.001	***
Treatment and Abrasion	2.565	0.055	.
Mixture, Time and Treatment	2.317	0.075	.
Mixture, Time and Abrasion	3.105	0.079	.
Mixture, Treatment and Abrasion	2.112	0.098	.
Time, Treatment and Abrasion	2.207	0.087	.
Mixture, Time, Treatment and Abrasion	0.584	0.626	

. $p < 0.1$, * $p < 0.05$, ** $p < 0.01$, *** $p < 0.001$

- The semiconductors TiO_2 ZnO applied by aqueous solution have no mechanical impact, assessed by Indirect Tensile Strength after water immersion.

The combination of TiO_2 with ZnO promoted the photocatalytic superhydrophobic and self-cleaning properties, providing the asphalt mixtures with these new capabilities. These functionalized pavement surfaces could degrade gases like SO_2 and NO_x, avoid accidents by removing the small dirt particles which are drained with water (lotus effect), degrade oils on the pavement surface and, additionally, it could prevent the pore clogging which happens in permeable asphalt mixtures. Great benefits to road safety and environment are foreseen with the construction of these layers.

Acknowledgments

This work was partially financed by FCT—Fundação para a Ciência e Tecnologia—under the project PTDC/FIS/120412/2010: "Nanobased concepts for Innovative & Eco-sustainable constructive material's surfaces" and project PEst-OE/ECI/UI4047/2014 supported by Portuguese Foundation for Science and Technology.

References

[1] M.M. Hassan, H. Dylla, S. Asadi, L.N. Mohammad, S. Cooper, Laboratory Evaluation of Environmental Performance of Photocatalytic Titanium Dioxide Warm-Mix Asphalt Pavements, J. Mater. Civ. Eng. 24 (2012) 599–605, https://doi.org/10.1061/(ASCE)MT.1943-5533.0000408.
[2] J.V.S. de Melo, G. Trichês, Evaluation of the influence of environmental conditions on the efficiency of photocatalytic coatings in the degradation of nitrogen oxides (NOx), Build. Environ. 49 (2012) 117–123, https://doi.org/10.1016/j.buildenv.2011.09.016.
[3] S. Bogutyn, C. Arboleda, A. Bordelon, P. Tikalsky, Rejuvenation techniques for mortar containing photocatalytic TiO<inf>2</inf> material, Constr. Build. Mater. 96 (2015) 96–101, https://doi.org/10.1016/j.conbuildmat.2015.07.192.
[4] X. Cao, X. Yang, H. Li, W. Huang, X. Liu, Investigation of Ce-TiO_2 photocatalyst and its application in asphalt- based specimens for NO degradation, Constr. Build. Mater. 148 (2017) 824–832, https://doi.org/10.1016/j.conbuildmat.2017.05.095.
[5] M. Saeli, D.M. Tobaldi, N. Rozman, A. Sever Škapin, J.A. Labrincha, R.C. Pullar, Photocatalytic nano-composite architectural lime mortar for degradation of urban pollutants under solar and visible (interior) light, Constr. Build. Mater. 152 (2017) 206–213, https://doi.org/10.1016/j.conbuildmat.2017.06.167.
[6] A. Arabzadeh, H. Ceylan, S. Kim, K. Gopalakrishnan, A. Sassani, S. Sundararajan, P.C. Taylor, Superhydrophobic coatings on Portland cement concrete surfaces, Constr. Build. Mater. 141 (2017) 393–401, https://doi.org/10.1016/j.conbuildmat.2017.03.012.
[7] S. Muzenski, I. Flores-Vivian, K. Sobolev, Hydrophobic engineered cementitious composites for highway applications, Cem. Concr. Compos. 57 (2015) 68–74, https://doi.org/10.1016/j.cemconcomp.2014.12.009.
[8] J.H.O. Nascimento, P. Pereira, E. Freitas, F. Fernandes, Development and characterization of a superhydrophobic and anti-ice asphaltic nanostructured material for road pavements, in: 7th Int. Conf. Maint. Rehabil. Pavements Technol. Control, At Auckland, New Zealand, 2003.
[9] A. Arabzadeh, H. Ceylan, S. Kim, K. Gopalakrishnan, A. Sassani, Superhydrophobic Coatings on Asphalt Concrete Surfaces, Transp. Res. Rec. J. Transp. Res. Board. 2551 (2016) 10–17, https://doi.org/10.3141/2551-02.
[10] B.N.J. Persson, U. Tartaglino, O. Albohr, E. Tosatti, Rubber friction on wet and dry road surfaces: the sealing effect, Phys. Rev. B - Condens. Matter Mater. Phys. 71 (2005) 1–8. doi:10.1103/PhysRevB.71.035428.
[11] Y. Hichri, V. Cerezo, Friction on road surfaces contaminated by fine particles : Some new experimental evidences (2017) 1–17, https://doi.org/10.1177/1350650117704345.
[12] J.O.O. Carneiro, S. Azevedo, V. Teixeira, F. Fernandes, E. Freitas, H. Silva, J. Oliveira, Development of photocatalytic asphalt mixtures by the deposition and volumetric incorporation of TiO_2 nanoparticles, Constr. Build. Mater. 38 (2013) 594–601, https://doi.org/10.1016/j.conbuildmat.2012.09.005.
[13] E. Bocci, L. Riderelli, G. Fava, M. Bocci, Durability of NO Oxidation Effectiveness of Pavement Surfaces Treated with Photocatalytic Titanium Dioxide, Arab. J. Sci. Eng. (2016) 1–7, https://doi.org/10.1007/s13369-016-2168-5.
[14] M. Chen, Y. Liu, NOx removal from vehicle emissions by functionality surface of asphalt road, J. Hazard. Mater. 174 (2010) 375–379, https://doi.org/10.1016/j.jhazmat.2009.09.062.
[15] D. Wang, Z. Leng, M. Hüben, M. Oeser, B. Steinauer, Photocatalytic pavements with epoxy-bonded TiO_2-containing spreading material, Constr. Build. Mater. 107 (2016) 44–51, https://doi.org/10.1016/j.conbuildmat.2015.12.164.
[16] M. Ni, M.K.H. Leung, D.Y.C. Leung, K. Sumathy, A review and recent developments in photocatalytic water-splitting using TiO_2 for hydrogen production, Renew. Sustain. Energy Rev. 11 (2007) 401–425, https://doi.org/10.1016/j.rser.2005.01.009.
[17] M.V. Diamanti, M. Ormellese, M. Pedeferri, Characterization of photocatalytic and superhydrophilic properties of mortars containing titanium dioxide, Cem. Concr. Res. 38 (2008) 1349–1353, https://doi.org/10.1016/j.cemconres.2008.07.003.
[18] J.S. Dalton, P.A. Janes, N.G. Jones, J.A. Nicholson, K.R. Hallam, G.C. Allen, Photocatalytic oxidation of NOx gases using TiO_2: A surface spectroscopic approach, Environ. Pollut. 120 (2002) 415–422, https://doi.org/10.1016/S0269-7491(02)00107-0.
[19] J. Zhao, X. Yang, Photocatalytic oxidation for indoor air purification: A literature review, Build. Environ. 38 (2003) 645–654, https://doi.org/10.1016/S0360-1323(02)00212-3.
[20] J. Chen, C. sun Poon, Photocatalytic construction and building materials: From fundamentals to applications, Build. Environ. 44 (2009) 1899–1906, https://doi.org/10.1016/j.buildenv.2009.01.002.
[21] V. Džimbeg-malčić, Ž. Barbarić-mikočević, K. Itrić, Kubelka-Munk Theory in Describing Optical Properties of Paper (I), Teh. Vjesn. 18 (2011) 117–124.
[22] H.G. Hecht, The Interpretation of Diffuse Reflectance Spectra, J. Res. Natl. Bur. Stand. Phys. Chem. 80a (1976) 567–583.
[23] C. Toro, B.T. Jobson, L. Haselbach, S. Shen, S.H. Chung, Photoactive roadways: determination of CO, NO and VOC uptake coefficients and photolabile side product yields on TiO_2 treated asphalt and concrete, Atmos. Environ. 139 (2016) 37–45, https://doi.org/10.1016/j.atmosenv.2016.05.007.
[24] A. Jager, R. Lackner, C. Eisenmenger-Sittner, R. Blab, Identification of Microstructural Components of Bitumen by Means of Atomic Force Microscopy (AFM), Proc. Appl. Math. Mech. 4 (2004) 400–401, https://doi.org/10.1002/pamm.200410.
[25] A.T. Pauli, J.F. Branthaver, C.M. Eggleston, R.E. Robertson, W. Grimes, Atomic Force Microscopy Investigation of Shrp Asphalts, in: Symp. Compat. Stab. Heavy Oils Residua, San Diego, California, 2001, pp. 1–11.
[26] H.L. Zhang, H.C. Wang, J.Y. Yu, Effect of aging on morphology of organo-montmorillonite modified bitumen by atomic force microscopy, J. Microsc. 92 (2010) 1–2, https://doi.org/10.1111/j.1365.
[27] W. Zhang, X. Xiao, X. Zeng, Y. Li, L. Zheng, C. Wan, Enhanced photocatalytic activity of TiO_2 nanoparticles using SnS2/RGO hybrid as co-catalyst: DFT study and photocatalytic mechanism, J. Alloys Compd. 685 (2016) 774–783, https://doi.org/10.1016/j.jallcom.2016.06.199.
[28] B. Madhukar, J. Wiener, J. Militky, S. Rwawiire, R. Mishra, K.I. Jacob, Y. Wang, B. M. Kale, J. Wiener, J. Militky, S. Rwawiire, R. Mishra, K.I. Jacob, Y. Wang, Coating of cellulose-TiO 2 nanoparticles on cotton fabric for durable photocatalytic self-cleaning and stiffness, Carbohydr. Polym. 150 (2016) 107–113, https://doi.org/10.1016/j.carbpol.2016.05.006.
[29] N.E. Altun, Incidental release of bitumen during oil shale grinding and impacts on oil shale beneficiation, Oil Shale. 26 (2009) 382–398, https://doi.org/10.3176/oil.2009.3.04.